Strain effects on point defects and chain-oxygen order-disorder transition in 123 cuprate compounds

Haibin Su*
Department of Materials Science and Engineering, SUNY at Stony Brook, Stony Brook, New York 11794, USA

David O. Welch†
Department of Materials Science, Brookhaven National Laboratory, Upton, New York 11973, USA

Winnie Wong-Ng‡
Ceramics Division, NIST, Gaithersburg, Maryland 20899, USA
(Received 22 March 2004; published 24 August 2004)

The energetics of Schottky defects in 123 cuprate superconductor series $R\mathrm{Ba_2Cu_3O_7}$ (where R = lanthandies) and $\mathrm{Y}A_2\mathrm{Cu_3O_7}$ (A = alkali earths), were found to have unusual relations if one considers only the volumetric strain. Our calculations reveal the effect of nonuniform changes of interatomic distances within the R-123 structures, introduced by doping homovalent elements, on the Schottky defect formation energy. The energy of formation of Frenkel pair defects, which is an elementary disordering event, in 123 compounds can be substantially altered under both stress and chemical doping. Scaling the oxygen-oxygen short-range repulsive parameter using the calculated formation energy of Frenkel pair defects, the transition temperature between orthorhombic and tetragonal phases is computed by quasichemical approximations (QCA's). The theoretical results illustrate the same trend as the experimental measurements in that the larger the ionic radius of R, the lower the orthorhombic/tetragonal phase transition temperature. This study provides strong evidence of the strain effects on order-disorder transition due to oxygens in the CuO chain sites.

DOI: 10.1103/PhysRevB.70.054517 PACS number(s): 74.25.Bt, 64.60.Cn, 61.10.−i

I. INTRODUCTION

It is well known that during the fabrication process of superconductor materials, a variety of point defects, such as substitution and interstitial impurities, vacancies, and cation-disorder are involved. These defects have a large effect on the properties of superconductors.[1] In type-II superconductors, high critical current densities can be achieved by the presence of high-density defects which will provide suitable pinning centers for the magnetic flux lines. The ideal size of defects for flux line pinning should be comparable to the superconducting coherence length. For cuprates such as $\mathrm{YBa_2Cu_3O_{7-\delta}}$ (Y-123), the coherence lengths are in the order of tens of Å while the conventional superconductors have a coherence length of several thousand Å. Thus atomic-scale structural inhomogeneities such as point defects and columnar defects can play an important role in flux-line pinning.[2] An increasing number of applications of the 123-type high-T_c superconductors use materials other than Y-123. For example, in many bulk forms and multilayer applications, Y is replaced by Nd, Sm, or other rare-earth (R) elements . Doping $\mathrm{YBa_2Cu_3O_{7-\delta}}$ with Ca, Sr, or other alkaline earth (A) elements has also been shown to improve bulk and grain boundary transport and other properties.[3–5]

Since it is well known that strain effects are important in the studies of point defects, it is expected that studies of strain effects on point defects for series of $R\mathrm{Ba_2Cu_3O_{7-\delta}}$ (R-123) compounds will be important for practical applications of superconductivity. In particular, the concentration and ordering of oxygen vacancies have significant effects on the superconducting properties. For Y-123, the superconducting temperature T_c depends on the oxygen stoichiometry. As an example of a generic doping curve in cuprates,[6,7] when δ is larger than around 0.7, the crystal loses superconductivity. However, if δ is smaller than 0.7, the compound is superconducting. It is generally believed that higher oxygen content can create more holes in the structure. When δ is between 0.1 and 0.7, the crystal is in the underdoped region, and T_c increases with increasing hole concentration. When the oxygen content is in the proper range, T_c is above the boiling point of liquid nitrogen. However, if more holes are created, the T_c value decreases instead, and the crystal is in an overdoped region.

Oxygen ordering in the Cu-O chains of the 123 structure gives rise to further complex structures.[8,9] Even when the average occupancies of oxygen sites remain constant, the occupation at chain and antichain sites can vary. Jorgensen *et al.*[10] observed that the superconducting transition temperature in Y-123 changes as a function of time following the quenching experiment while the oxygen content is fixed. This demonstrates that the specific ordering of the oxygen atoms in the basal plane is another important parameter that controls T_c in the Y-123 system.[11] The ordering process in the Cu-O chain is the origin of the structural transition between tetragonal and orthorhombic phases in the 123 structure, which has been extensively studied since the discovery of Y-123.[12–15] Structural transition of Y-123 is strongly affected by external pressure as well.[16–19] In addition, there are systematic results reported by Wong-Ng and co-workers[20–22] showing that the orthorhombic/tetragonal phase transition temperatures in R-123 can be scaled approximately linearly with the ionic radius of R^{3+}. The above experimental obser-

vations indicate that lattice strain may play an important role in phase transition, which has not been investigated theoretically and systematically so far.

In this paper, we plan to study the effects of homovalent substitutions at Y and Ba sites, and hydrostatic pressure on the order-disorder transition theoretically. Considering large stress fields due to dislocations around grain boundaries, this study will also provide valuable information for understanding the transport properties in the vicinity of grain boundaries. First we briefly explain methods used in atomistic simulations. Secondly, we focus on the effects of strain on Schottky defects and related phenomena for a series of homovalent substitutions at Y and Ba sites of $YBa_2Cu_3O_{7-\delta}$. Although the 123 structure is not stable in the Ca and Sr analogs under ambient pressure,[23–25] partial substitution of Sr on the Ba site has been reported.[4,23,26–28] Finally, strain effects on chain-oxygen order-disorder transition of $RBa_2Cu_3O_{7-\delta}$ will be investigated.

II. ATOMISTIC SIMULATION METHODS

Since the parent compounds of high-T_c cuprate superconductors can be considered as charge-transfer insulators, ionic bonding can be assumed to have a large contribution to the lattice energy. Methods used to study atomistic phenonmena in conventional oxides can therefore be applied to study cuprates. The cuprates become superconductors at a proper doping level and temperature. However, the charge carrier density is very low compared with that of conventional metals. In addition, the charge carriers are confined within copper-oxygen planes. Consequently, the screening effect is not as strong as that of conventional metals. The lattice energy calculated from ionic models is somewhat overestimated. The point defect's energy is also slightly overestimated due to the omission of screening effect in metallic region of the phase diagram, which can be improved by including polarization effects in the shell model.[29] Many previous theoretical investigations are based on this type of ionic model (for example, see Refs. 30–34).

Several pair-potential sets of shell model parameters have been determined for Y-123 by Baetzold.[31,32] To systematically study homovalent substitutions on Y and Ba sites, a consistent set of shell model parameters using the data set for $YBa_2Cu_3O_7$ (Ref. 31) was further developed to account for the dependence of the Born repulsion of the two ions on their net charges, on outer electronic configurations,[35,36] and on the common "r^3 law" between polarizability and radius.[37] The "virtual crystal method" is applied here to interpret experimental data of mixing two types of elements on one site. This method essentially is, for the purpose of calculating average structural and elastic properties, to approximate the mixture of two ions distributed over one sublattice by identical average "virtual ions." It allows the incorporation of compositional changes at the atomic level, but ignores explicit effects of disorder. For instance, when Ba^{2+} is partially replaced by Sr^{2+} in experiments, the composition-weighted average value of the two ions' radii is taken to approximate that of each virtual divalent ion. After constructing a consistent interatomic pair potential set,[38] we used the "general utility lattice program" (GULP),[39] which integrates the above modeling methods at an atomistic scale, to study lattice energy, elastic constants, and lattice dynamic properties. In summary, our calculations are based on short-range potentials of the Buckingham-type, long-range Coulomb potentials, and displacement-induced deformations of the electronic charge density in the framework of a shell model.

III. SCHOTTKY DEFECTS IN 123 COMPOUNDS

Any deviation in a crystal from a perfect structure is an imperfection. The simplest imperfection is a lattice vacancy, which is a missing atom or ion, known as a Schottky defect. Schottky defects involve "multiple" vacancies while preserving electrical neutrality. Regardless of how a Schottky defect is created, it is necessary to expend a certain amount of work per atom to take it to the surface. We calculated point defect energy by the Mott-Littleton approach.[40,41] Some vacancies are at anionic sites and others at the cationic sites. For Y-213, the defect reaction is given as follows:

$$YBa_2Cu_3O_7 \rightarrow V_Y^{-3} + 2V_{Ba}^{-2} + 3V_{Cu}^{-2} + 7V_O^{+13/7}; \qquad (1)$$

where V represents a vacancy. According to mass action law, the equilibrium constant (K) at a finite temperature can be written as

$$K = c(V_Y^{-3})c(V_{Ba}^{-2})^2c(V_{Cu}^{-2})^3c(V_O^{+13/7})^7 = \bar{c}^{13}, \qquad (2)$$

where c is the equilibrium concentration of vacancies and $\bar{c}$ is the average concentration of vacancies. The equilibrium concentration of the vacancy j, c_j, can be computed from Boltzmann statistics as

$$c_j = N_j \exp\left(\frac{-E_{v_j}}{kT}\right), \qquad (3)$$

where N_j is the number of atom j per unit volume and E_{v_j} is the energy required to take atom j from its lattice site inside the crystal to a site on the surface. Substituting the equilibrium concentraions of vacancies into Eq. (2), we obtain the expression for the average concentration of vacancies $\bar{c}$ as follows:

$$\bar{c} = N \exp\left(\frac{-\bar{E}_{\text{Schottky}}}{kT}\right), \qquad (4)$$

where N is the number of formula units per unit volume and $\bar{E}_{\text{Schottky}}$ is given, in terms of the formation energy of individual vacancy (an ion is removed to infinity instead of the surface of crystals) and lattice energy E^{lattice}, as

$$\bar{E}_{\text{Schottky}} = \frac{\sum_i E_i^{\text{vacancy}} + E^{\text{lattice}}}{13}. \qquad (5)$$

In R-123, the absolute value of site potential decreases continuously with increasing ion radius at the Y site, which is consistent with applying external tensile pressure. Usually, the change of short-range repulsion is less significant than that of the Madelung site potential. In general, the smaller absolute site potential value is favorable for lowering va-

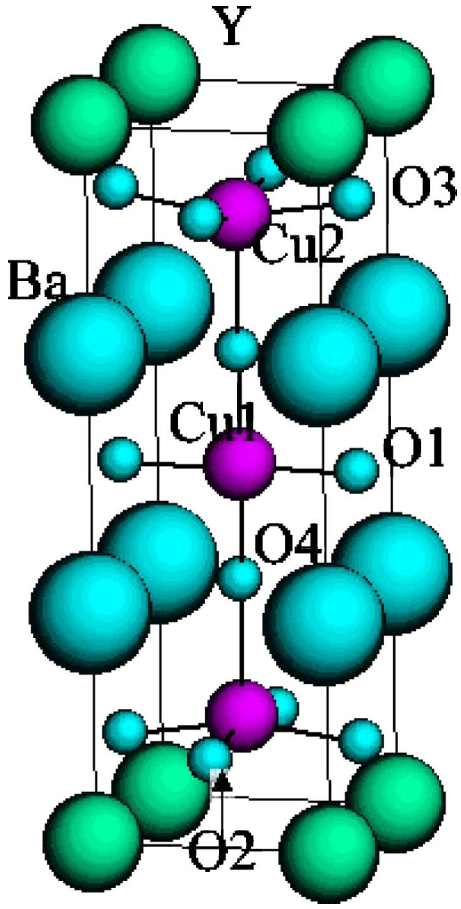

FIG. 1. Crystal structure of $YBa_2Cu_3O_7$.

cancy energy, and vice versa. Furthermore, an increase of the total volume leads to the expansion of effective relaxation space so that the vacancy energy can further decrease due to the relaxation of the atoms. In the shell model, the electronic polarization due to the electronic relaxation also lowers the defect energy. In $YA_2Cu_3O_7$ (*A*-123), as the radius of the ion at *A* sites becomes larger, a similar phenomenon is observed. In both $RBa_2Cu_3O_7$ and $YA_2Cu_3O_7$, the lower Schottky defects formation energies are always associated with the larger volume. This indicates that the volume of formation of Schottky defects is positive, or the volume of the entire crystal expands during the formation of Schottky defects.

As shown in Fig. 1, the complex structure of 123 compounds can be roughly divided into six layers along the *c* axis direction: *R*-CuO_2(Cu2)-BaO-CuO(Cu1)-BaO-CuO_2-*R*. For the sake of simplicity, the distances between planes are represented by the separations of cations projected along the *c* axis. The external and internal strains are computed with Y-123 as a reference. Replacing Y^{3+} by larger R^{3+} ions leads to positive external strains, indicating the dimensions of the cell expand as increasing *R* size. The more interesting observations are the changes of internal parameters within the unit cell. The variance of internal strains provide direct information of the changes of layers' separations in *R* series. The interatomic distances vary quite differently with ionic radius in the *R*-123 and *A*-123 series.[38] For instance, the distance of *R*-CuO_2 becomes larger with increasing *R* size, which is expected from the change of short-range repulsion of *R*-O. However, even when the entire cell volume increases as the *R* ion becomes larger, some parts of unit cell contract such as interlayer separations between CuO_2(Cu2)-BaO and BaO-CuO(Cu1) (or, bond lengths of Cu2-O4 and Cu1-O4). Consequently, the average energy of the point defect only decreases slightly because of the existing compressive blocks within the structure as plotted in Fig. 1. In the *A*-123 series, when Ba^{2+} is (partially) replaced by smaller A^{2+}, the variances of external and internal strains are of the same sign, reflecting a somewhat "even" expansion of the entire structure. The difference between *R*-123 and *A*-123 is reflected by the changes of *A*-*A* and Cu1-Cu2 distances. Unlike those in *R*-123, for *A*-123 both distances become larger with increasing *A* size. The different changes of internal strains due to doping at either Y or Ba sites governs the absolute value of slope of Schottky defects of *R*-123 and *A*-123 (see Fig. 2). In the previous studies,[42] they found interesting correlations between dopant radius and energy of solution in $YBa_2Cu_3O_7$. The trend of subsituting divalent cation for barium matches well with that in the Schottky defect energy of $YA_2Cu_3O_7$. However, there exist clear different trends between replacing yttrium by trivalent ions in $YBa_2Cu_3O_7$ and that in the Schottky defect energy of $RBa_2Cu_3O_7$. The reason is that the parent structure is fixed for former case, so that the trivalent ion larger than yttrium leads to more energy of solution. One the other hand, the Schottky defect has to consider all the atoms in the unit cell. Unless the structures change more or less "homogeneously," the energy of solution at one specific site may evolve differently from the Schottky defect energy.

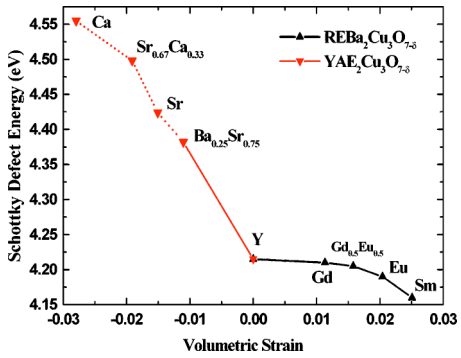

FIG. 2. Schottky defects formation energy vs volumetric strain. The volumetric strain is defined as $(V-V_0)/V_0$, where V_0 is the volume of Y-123 compound. All volumes are obtained by optimizing cell parameters and internal coordinates to minimize the total energy. The solid solutions are treated by the "virtual crystal method."

Recall that the relation between cell volume, bulk modulus of *R*-123, and the trend of thermal expansion coefficients are also the manifestation of the complexity of the 123 structure.[38] There is an "unusual" relation between Schottky defects formation energy and $B\Omega$ (where B is bulk modulus and Ω is the mean volume per atom) of *R*-123 in Fig. 3. As reported by Varotsos,[43] the Schottky defects formation energy is proportional to $B\Omega$ for elemental and binary crystals. While this relation appears to be obeyed by the *A*-123 series, it is violated by the *R*-123 series. The possible reason is still

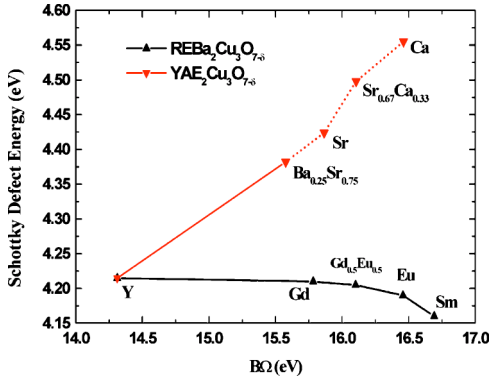

FIG. 3. Schottky defects formation energy vs $B\Omega$ of 123 compounds. B is the bulk modulus and Ω is the mean volume per atom of 123 compounds. Both B and Ω are calculated from the optimized structures with minimal total energy. The solid solutions are treated by the "virtual crystal method."

the non-uniform changes of the interatomic distances within the unit cell for R-123. We have studied the trend of melting temperature of R-123 by "Lindemann law,"[44,45] and found that the vibrations along the c axis are the most important modes to determine the melting temperatures while the isotropic approximation fails to yield correct results.[38] Here, we take another approach to investigate the relation between melting temperatures and formation energies of Schottky defects. Kurosawa[46] gave a direct correlation between them, which is listed in Table I. While it appears that a smaller Schottky defect formation energy can lower the melting temperature of simple binary significantly, it has not been proved to be true for compounds with complex structure. Note that the predominant point defect could be Frenkel defect rather than Schottky defect in some complex structures. However, Schottky defect energy provides an unambiguous measure on the average cohesive strength. For example, despite the Schottky defect formation energy of Sm-123 is smaller than that of Y-123, Sm-123 has a higher melting temperature. It is necessary to study internal strains rather than volumetric strains in order to obtain a detailed analysis of the thermodynamic properties of compounds with complex structures. In general, we found that the signs of the slopes $(dE_{\text{Schottky}}/d\epsilon_v)$ of R-123 and A-123 in Fig. 2 are the same. The difference between these two slopes and the "unusual" relationships between Schottky defects formation energies and $B\Omega$ and melting temperatures of R-123 compounds all reflect the complexity of the crystal structure.

IV. CHAIN-OXYGEN ORDER-DISORDER TRANSITION

The oxygen content is an important parameter for superconductivity in cuprates. In addition, the distribution (ordering) of oxygen atoms among the atomic sites strongly affects T_c. The order-disorder transition of chain oxygen has been extensively studied both experimentally and theoretically.[8,9,12–15] Raman studies show that there exists a pressure-induced ordering phenomenon.[19] The strain effect on this transition has not been investigated theoretically in a systematic fashion. Here we focus on the effects of homo valent substitutions at Y and Ba sites, and hydrostatic pressure on the order-disorder transition.

In the quasi chemical approximation (QCA),[12,15] the short-range order is characterized by the fraction number of near-neighbor pair sites occupied by oxygen-oxygen pairs $p=N_{oo}/4N$, where N is the number of sites on each of the sublattice α and β, and N_{oo} is the number of oxygen-oxygen near neighbor pairs. The long-range order parameter S is defined such that the fractional site occupancy on sublattice β is $c(1+S)$, while that on sublattice α is $c(1-S)$ where c is the fractional site occupancy averaged over both sublattices. (Note that for $YBa_2Cu_3O_{7-\delta}$, c is 0.5 when δ is zero; i.e., $\delta=1-2c$.)

The partition function is given by

$$Z(T)=\sum_{R_\alpha}\sum_{q_{\alpha\alpha}} g(R_\alpha,q_{\alpha\alpha})e^{-W(R_\alpha,q_{\alpha\alpha})/kT}, \tag{6}$$

where $R_\alpha=N(1+S)/4$, $q_{\alpha\alpha}$ is the probability of pairs $\alpha\alpha$, and $g(R_\alpha,q_{\alpha\alpha})$ is proportional to the total number of ways one can divide N entities into four groups of $\alpha\alpha,\alpha\beta,\beta\alpha$, and $\beta\beta$ pairs. The configuration energy is denoted as $W(R_\alpha,q_{\alpha\alpha})$. As usual, we may replace each sum by its maximum term in the summation for the system of a great many assemblies. Hence, we have

$$Z(T)=\sum_{R_\alpha} g(R_\alpha,\bar{q}_{\alpha\alpha})e^{-W(R_\alpha,\bar{q}_{\alpha\alpha})/kT}, \tag{7}$$

in which the most probable value $\bar{q}_{\alpha\alpha}$ of $q_{\alpha\alpha}$ is determined by

$$\frac{\partial}{\partial \bar{q}_{\alpha\alpha}}\left(\ln g(R_\alpha,\bar{q}_{\alpha\alpha})-\frac{W(R_\alpha,\bar{q}_{\alpha\alpha})}{kT}\right)=0. \tag{8}$$

There are three unknowns for a given value of temperature T and oxygen partial pressure P_{O_2}: c,S,p. Three equations involving these three unknowns are obtained by requiring that (1) the chemical potential of oxygen atoms is the same on both sublattices, (2) the chemical potential of oxygen atoms is the same in the solid and in the gas phase (which consists mostly of diatomic molecules but has an equilibrium concentration of atomic oxygen), and (3) the free energy of the system is a minimum with respect to the fractional number of oxygen-oxygen pairs. The following deri-

TABLE I. The Schottky defects formation energy and melting temperature of binary and R-123 compounds. The data of binary compounds are from Ref. 46. The melting temperature data of R-123 are from Ref. 47.

Crystal	NaF	NaCl	NaBr	MgO	CaO	SrO	Crystal	YBCO	GdBCO	EuBCO	SmBCO
$\bar{E}_{\text{Schottky}}$(eV)	2.5	2.2	2.0	6.3	5.5	5.0	$\bar{E}_{\text{Schottky}}$(eV)	4.22	4.21	4.20	4.16
T_{melting}(K)	1259	1073	1018	3070	2850	2700	T_{melting}(K)	1250	1290	1300	1325

vations follow the similar procedure as described in Ref. 48. Using the above conditions, QCA yields

$$\ln\left(\frac{c(1+S)-p}{c(1-S)-p}\right)=\frac{3}{4}\ln\left(\frac{(1+S)[1-c(1-S)]}{(1-S)[1-c(1+S)]}\right), \quad (9)$$

$$\ln\left[\left(\frac{1-c(1+S)}{c(1+S)}\right)^3\left(\frac{c(1+S)-p}{1-2c+p}\right)^4\right] = \ln\left[\left(\frac{P_{O_2}}{\xi}\right)^{1/2}\frac{1}{(kT)^{7/4}}\right]-\frac{\epsilon+1/2E_d}{kT}, \quad (10)$$

$$\frac{v}{kT}=\ln\left(\frac{[c(1+S)-p][c(1-S)-p]}{p(1-2c+p)}\right), \quad (11)$$

where ϵ is the energy to remove an oxygen atom from the gas and place it in the lattice, v is the repulsion energy between near-neighbor oxygens, E_d is the dissociation energy of one oxygen molecule, ξ is equal to 4.144×10^{19} Pa(eV)$^{-7/2}$. The desired values of c, S, and p are obtained for given values of T and P_{O_2}, by simultaneously solving the above equations. We note that the order-disorder transition temperature T_{od} is related to the oxygen-oxygen repulsion energy v and the value of the average site occupancy c at this temperature by

$$\frac{v}{kT_{OD}}=\ln\left(\frac{16c(1-c)}{1-4(1-2c)^2}\right). \quad (12)$$

Frenkel defects involve an atom displaced from its normal site into an interstitial site. If the interstitial site is chosen as antichain site for 123 compounds, this Frenkel pair is closely related to chain-oxygen order-disorder transition. Forming a Frenkel pair in an otherwise perfect crystal is an elementary disordering event. As the disordering proceeds, it is important to account for defect-defect interactions. Using Mott-Littleton approach, we have computed the isolated Frenkel pair formation energy for RBa$_2$Cu$_3$O$_7$, YA_2Cu$_3$O$_7$, and Y-123 under hydrostatic pressure. We found that this formation energy increases in compressive regions and decreases in tensile regions under hydrostatic pressure. This is the origin of ordering under stress. From the systematic investigation of the phonon spectral characteristics with the application of pressure,[19] it was observed that the changes induced by the hydrostatic pressure have a strong effect on chain ordering. Results of our calculations are consistent with the reported observation. Figure 4 shows the plots of the Frenkel pair formation energy versus lattice strain (volumetric strain) for both the R series and the A series. These two plots demonstrate a similar trend and they form a well-connected smooth curve. The similar behavior of the curve for the R and A series (with chemical doping) and the curve for Y-123 (with hydrostatic pressure) indicates that the oxygen disordering energy is dominated by lattice strain, which is expected if the short range repulsion terms dominate the energy required to form the oxygen interstitial ion.

Furthermore, scaling the oxygen-oxygen short-range repulsive energy by the calculated Frenkel Pair formation energy, the transition temperature between orthorhombic and tetragonal phases is computed based on Eq. (12). The transition temperature of YBa$_2$Cu$_3$O$_{7-\delta}$ was used as a reference. The results are plotted in Fig. 5 with the experimental data taken from Refs. 20–22. There exists observable difference (around 100 K) between theory and experiment in the Nd-123 system.[22] It has been determined experimentally that the orthorhombic-to-tetragonal phase transition in the R-123 series take place at an oxygen composition in the range of 6.4 (Er) to 6.83 (Nd), not all at 6.5 (Y).[20–22] The change of oxygen content leads to the change of structure such as lattice parameters and atomic positions,[8,9] which in turn alters the formation energy of Frenkel pairs. Since we set the reference transition temperature to be the value in Y-123 case, this corresponds to the transition at oxygen content being 6.5. If we track the whole process of order-disorder transition starting from fully oxygenated case, the total oxygen content decreases until the transition is finished. The formation energy of Frenkel pairs decreases also as anisotropy in the ab plane [defined as $(b-a)/a$] reduces. Note that the transition occurs at oxygen content being 6.83 in a Nd-123 system, this indicates the anisotropy in Nd-123 remains higher compared with Y-123. Therefore, the formation energy of Frenkel pairs

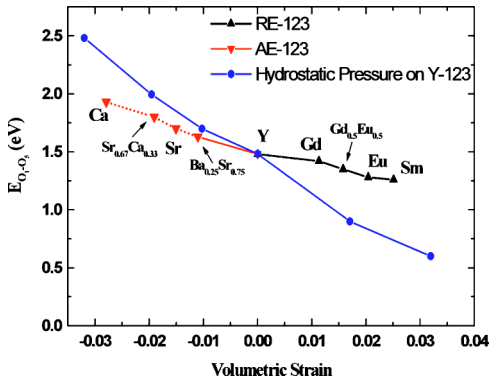

FIG. 4. Frenkel pair formation energy vs volumetric strain for 123 compounds. The energy corresponds to moving one chain oxygen into an antichain site. All volumes are obtained by optimizing cell parameters and internal coordinates to minimize the total energy. The solid solutions are treated by the "virtual crystal method."

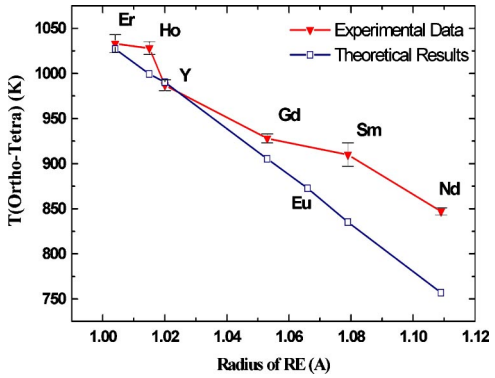

FIG. 5. Chain-oxygen order-disorder transition temperature of RBa$_2$Cu$_3$O$_7$. The theoretical data are calculated by using the transition temperature of YBa$_2$Cu$_3$O$_{7-\delta}$ as a reference. The experimental data are from Refs. 20–22. The error bars indicate the temperature range measured by x-ray diffraction.

decreases less than that in Y-123 during the whole process of transition as observed experimently. This means that in our "simple" model the transition temperature for Nd-123 is underestimated. But, the remarkable thing is that using such a simple model, the trend of the theoretical results agree well with the experimental measurements. It is seen that stress and "chemical pressure" can substantially alter the degree of disorder. This study provides a clear evidence for the effects of strain on order-disorder transition. Previous studies also show there are quite rich microstructures resulting from this orthorhombic-to-tetragonal phase transition: for instance, twin structures and related twinning dislocations,[49,50] tweed morphology caused mainly by (110) and $(\bar{1}10)$ shear displacements.[1] In particularly, our results can be applied further to deduce that strain near edge dislocations in low angle grain boundaries,[51] which can also have a significant effect on the degree of ordering in cuprate materials. For example, the interactions between point defects and strain fields due to dislocations and/or grain boundaries can affect the distribution of point defects, and the content and degree of order of oxygen atoms.[38]

V. CONCLUSIONS

Based on the Mott-Littleton approach we studied the Schottky defect formation energy in the 123 phase as a function of volumetric strain. Generally, a more expanded lattice favors a lower Schottky defect formation energy, and vice verse. The difference of slopes $(d\mathrm{E}_{\mathrm{Schottky}}/d\epsilon)$ between *R*-123 and $YA_2Cu_3O_{7-\delta}$, the "unusual" relation between Schottky defects formation energies and $B\Omega$ and melt temperatures of *R*-123 compounds all reflect the complexity of the crystal structure of 123 compounds.

Our study also illustrates the importance of strain effects on the orthorhombic/tetragonal phase transition in the *R*-123 compounds. We have calculated the formation energy of Frenkel pair defects as a function of volumetric strain for $RBa_2Cu_3O_7$ and $YA_2Cu_3O_7$, and for $YBa_2Cu_3O_7$ under hydrostatic pressure. Our calculations show good agreement with experimental observations in that pressure favors ordering of the CuO chains. For example, the Frenkel pair formation energy indeed increases significantly (around -0.25 eV/0.01 volumetric strain) under compression. Based on a quasichemical approach, the orthorhombic/tetragonal transition temperatures for *R*-123 have been computed by scaling the effective oxygen-oxygen short-range repulsive energy in the CuO chain using the Frenkel pair formation energy. The calculated results agree with experimental data in that the larger the ionic size of *R*, the lower the orthorhombic/tetragonal phase transition temperature.

ACKNOWLEDGMENTS

The work at NIST was partially supported by the U.S. Department of Energy (DOE). The work at Brookhaven National Laboratory was performed under the auspices of the Division of Materials Sciences, Office of Science, U.S. Department of Energy under Contract No. DE-AC-02-98CH10886.

*Present address: Beckman Institute 139-74, California Institute of Technology, Pasadena, CA 91125. Electronic address: hbsu@wag.caltech.edu

†Electronic address: dwelch@bnl.gov

‡Electronic address: winnie.wong-ng@nist.gov

[1] Z. X. Cai and Y. Zhu, *Microstructures and Structural Defects in High-Temperature Superconductors* (World Scientific, Singapore, 1998).

[2] P. D. Yang and C. M. Lieber, Science **273**, 1836 (1996).

[3] J. B. Langhorn, M. A. Black, and P. J. McGinn, Mater. Lett. **41**, 289 (1999).

[4] F. Licci, A. Gauzzi, M. Marezio, G. P. Radaelli, R. Masini, and C. Chaillout-Bougerol, Phys. Rev. B **58**, 15 208 (1998).

[5] H. Hilgenkamp and J. Mannhart, Rev. Mod. Phys. **74**, 485 (2002).

[6] H. B. Zhang and H. S. Sato, Phys. Rev. Lett. **70**, 1697 (1993).

[7] J. L. Tallon, C. Bernhard, H. Shaked, R. L. Hitterman, and J. D. Jorgensen, Phys. Rev. B **51**, 12 911 (1995).

[8] R. J. Cava, B. Batlogg, C. H. Chen, E. A. Rietman, S. M. Zahurak, and D. Werder, Nature (London) **329**, 423 (1987).

[9] R. J. Cava, B. Batlogg, C. H. Chen, E. A. Rietman, S. M. Zahurak, and D. Werder, Phys. Rev. B **36**, 5719 (1987).

[10] J. D. Jorgensen, S. Pei, P. Lightfoot, H. Shi, A. P. Paulikas, and B. W. Veal, Physica C **167**, 571 (1990).

[11] H. F. Poulsen, N. H. Andersen, J. V. Andersen, H. Bohr, and O. G. Mouritsen, Nature (London) **349**, 594 (1991).

[12] H. Bakker, D. O. Welch, and O. W. Lazareth, Solid State Commun. **64**, 237 (1987).

[13] D. Defontaine, L. T. Wille, and S. C. Moss, Phys. Rev. B **36**, 5709 (1987).

[14] A. G. Khachaturyan, S. V. Semenovskaya, and J. W. Morris, Phys. Rev. B **37**, 2243 (1988).

[15] H. Bakker, J. P. A. Westerveld, D. M. R. Locascio, and D. O. Welch, Physica C **157**, 25 (1989).

[16] W. H. Fietz, R. Quenzel, H. A. Ludwig, K. Grube, S. I. Schlachter, F. W. Hornung, T. Wolf, A. Erb, M. Klaser, and G. MullerVogt, Physica C **270**, 258 (1996).

[17] S. Sadewasser, Y. Wang, J. S. Schilling, H. Zheng, A. P. Paulikas, and B. W. Veal, Phys. Rev. B **56**, 14 168 (1997).

[18] S. Sadewasser, J. S. Schilling, A. P. Paulikas, and B. W. Veal, Phys. Rev. B **61**, 741 (2000).

[19] E. Liarokapis, D. Lampakis, T. Nishizaki, and C. Panagopoulos, High Press. Res. **18**, 109 (2000).

[20] W. Wong-Ng, L. P. Cook, C. K. Chiang, L. Swartzendruber, and L. H. Bennett, in *Advances in Ceramic Materials and Ceramic Superconductor II*, edited by M. F. Yan (American Ceramic Society, Westerville, OH, 1988), Vol. II, p. 27.

[21] W. Wong-Ng, L. P. Cook, C. K. Chiang, M. D. Vaudin, D. L. Kaiser, F. Beech, L. Swartzen-druber, L. H. Bennett, and E. R. Fuller, Jr., in *High Temperature Superconducting Compounds:*

Processing & Related Properties, edited by S. H. Whang and A. DasGupta (The Minerals, Metals and Materials Society, Warrendale, PA, 1989), Vol. II, p. 553.
[22] W. Wong-Ng, L. P. Cook, H. B. Su, D. O. Welch, C. K. Chiang, and L. Bennett (unpublished).
[23] R. S. Roth, C. J. Rawn, J. D. Whitler, C. K. Chiang, and W. K. Wong-Ng, J. Am. Ceram. Soc. **72**, 395 (1989).
[24] B. Okai, Jpn. J. Appl. Phys., Part 2 **29**, L2180 (1990).
[25] P. K. Davies, E. Caignol, and T. King, J. Am. Ceram. Soc. **74**, 569 (1991).
[26] Y. Cao, T. L. Hudson, Y. S. Wang, S. H. Xu, Y. Y. Xue, and C. W. Chu, Phys. Rev. B **58**, 11 201 (1998).
[27] H. G. Lee, A. P. Litvinchuk, M. V. Abrashev, M. N. Iliev, S. H. Xu, and C. W. Chu, J. Phys. Chem. Solids **59**, 1994 (1998).
[28] M. Marezio, E. Gilioli, P. G. Radaelli, A. Gauzzi, and F. Licci, Physica C **341**, 375 (2000).
[29] B. G. Dick and A. W. Overhauser, Phys. Rev. **112**, 90 (1958).
[30] S. L. Chaplot, Phys. Rev. B **37**, 7435 (1988).
[31] R. C. Baetzold, Phys. Rev. B **38**, 11 304 (1988).
[32] R. C. Baetzold, Phys. Rev. B **42**, 56 (1990).
[33] S. Valkealahti and D. O. Welch, Physica C **162**, 540 (1989).
[34] N. F. Wright and W. H. Butler, Phys. Rev. B **42**, 4219 (1990).
[35] L. Pauling, Z. Kristallogr. **67**, 377 (1928).
[36] M. P. Tosi, Solid State Phys. **16**, 1 (1964).
[37] K. D. Bonin and V. V. Kresin, *Electric-Dipole Polarizabilities of Atoms, Molecules, and Clusters* (World Scientific, Singapore, 1997).
[38] H. B. Su, Ph.D. thesis, SUNY at Stony Brook, 2002.
[39] J. D. Gale, J. Chem. Soc., Faraday Trans. **93**, 629 (1997).
[40] N. F. Mott and M. J. Littleton, Trans. Faraday Soc. **34**, 485 (1938).
[41] N. F. Mott and R. W. Gurney, *Electronic Processes in Ionic Crystals* (Oxford University Press, Oxford, 1948).
[42] M. S. Islam and R. C. Baetzold, Phys. Rev. B **40**, 10 926 (1989).
[43] P. Varotsos and W. Ludwig, Phys. Rev. B **18**, 2683 (1978).
[44] J. J. Gilvarry, Phys. Rev. **102**, 308 (1956).
[45] J. P. Poirier, *Introduction to the Physics of the Earth's Interior* (Cambridge University Press, Cambridge, 1991).
[46] T. Kurosawa, J. Phys. Soc. Jpn. **12**, 338 (1957).
[47] K. Osamura and W. Zhang, Z. Metallkd. **84**, 522 (1993).
[48] T. Muto and Y. Takagi, Solid State Phys. **1**, 194 (1955).
[49] V. S. Boyko, S. W. Chan, and M. Chopra, Phys. Rev. B **63**, 224521 (2001).
[50] S. W. Chan and V. S. Boyko, Phys. Rev. B **53**, 16 579 (1996).
[51] H. Kung, J. P. Hirth, S. R. Foltyn, P. N. Arendt, Q. X. Jia, and M. P. Maley, Philos. Mag. Lett. **81**, 85 (2001).